Projected-Wave-Function Study of the Spin-1/2 Heisenberg Model on the Kagomé Lattice

Ying Ran, Michael Hermele, Patrick A. Lee, and Xiao-Gang Wen

Department of Physics, Massachusetts Institute of Technology, Cambridge, Massachusetts 02139, USA

(Received 21 November 2006; published 16 March 2007)

We perform a Gutzwiller projected-wave-function study for the spin-1/2 Heisenberg model on the Kagomé lattice to compare energies of several spin-liquid states. The result indicates that a U(1)-Dirac spin-liquid state has the lowest energy. Furthermore, even without variational parameters, the energy turns out to be very close to that found by exact diagonalization. We show that such a U(1)-Dirac state represents a quantum phase whose low-energy physics is governed by four flavors of two-component Dirac fermions coupled to a $U(1)$ gauge field. These results are discussed in the context of recent experiments on $ZnCu_3(OH)_6Cl_2$.

DOI: 10.1103/PhysRevLett.98.117205 PACS numbers: 75.10.Jm, 75.50.Ee

Recent experimental studies of a spin-1/2 Kagomé system $ZnCu_3(OH)_6Cl_2$ [1–3] show that the system is in a nonmagnetic ground state. The Kagomé lattice can be viewed as corner-sharing triangles in two dimensions [Fig. 1(a)]. The compound shows no magnetic order down to very low temperature (50 mK) compared with the Curie-Weiss temperature (>200 K). The spin susceptibility rises with decreasing temperature, but saturates to a finite value below 0.3 K. The specific heat is consistent with a linear T behavior below 0.5 K. There is no sign of a spin gap in dynamical neutron scattering. These observations led us to reexamine the issue of the ground state of the spin-1/2 Kagomé lattice.

Based on Monte Carlo studies of Gutzwiller projected wave functions, we propose the ground state to be a U(1)-Dirac spin-liquid state which has relativistic Dirac spinons. The low-energy effective theory is a U(1) gauge field coupled to four flavors of two-component Dirac fermions in $2+1$ dimension. This state was studied earlier in the mean-field approximation [4]. However, that study focused on an instability toward a valence bond solid (VBS) state which breaks translation symmetry [4]; it was not appreciated that the U(1)-Dirac state can be a stable phase. Using the projective symmetry group [5–7] (PSG) technique, we reconsider the stability of the U(1)-Dirac state and find it can be stable. Our numerical calculations confirm that neighbor states like the VBS states and chiral spin-liquid state all have higher energies.

One way to construct spin-liquid states is to introduce fermionic spinon operators [8,9] $f_\uparrow$ and $f_\downarrow$ to represent the bosonic spin operator: $\vec{\mathbf{S}}_i = \frac{1}{2} f^\dagger_{i\alpha} \vec{\sigma}_{\alpha\beta} f_{i\beta}$. This representation enlarges the Hilbert space, and a local constraint is needed to go back to the physical Hilbert space: $f^\dagger_\uparrow f_\uparrow + f^\dagger_\downarrow f_\downarrow = 1$. For the nearest neighbor Heisenberg model (with antiferromagnetic exchange $J > 0$)

$$H = J \sum_{\langle ij \rangle} \vec{\mathbf{S}}_i \cdot \vec{\mathbf{S}}_j, \tag{1}$$

we can substitute the spin operator by the spinon operators, so that the spin interaction is represented as a four-fermion interaction. The four-fermion interaction can be decomposed via a Hubbard-Stratonovich transformation by introducing the complex field χ_{ij} living on the links. The path integral of the spin model is then $Z = \int d\chi d\lambda df df^\dagger e^{-S}$, where the action is

$$S = \int d\tau \Big[\sum_i f^\dagger_{i\alpha} \partial_\tau f_{i\alpha} + i\lambda_i (f^\dagger_{i\alpha} f_{i\alpha} - 1) \times \sum_{ij} 2J|\chi_{ij}|^2 + J(\chi_{ij} f^\dagger_{j\alpha} f_{i\alpha} + \text{H.c.}) \Big]. \tag{2}$$

Here λ is the Lagrangian multiplier to ensure the local constraint, and it can be viewed as the time component of a compact U(1) gauge field, whereas the phase of χ_{ij} can be viewed as the space components of the same gauge field. Only when the full gauge field fluctuations are included can one go back to the physical Hilbert space.

With this fermionic representation, one can do a mean-field study of the spin-liquid states by taking χ_{ij} as mean-field parameters. For the Kagomé lattice, the mean-field states are characterized by the fluxes through the triangles and the hexagons. Controlled mean-field studies were done by generalizing the $SU(2)$ spin model to $SU(N)$ spin model via introducing $N/2$ flavors of fermions [4,10], and several candidate states were found: (i) VBS states which break translation symmetry. (ii) A spin-liquid state (SL-[$\frac{\pi}{2}$, 0]) with a flux $+\pi/2$ through each triangle on Kagomé lattice and zero flux through the hexagons. This is a chiral spin liquid which breaks time-reversal symmetry. (iii) A spin-liquid state (SL-[$\pm\frac{\pi}{2}$, 0]) with staggered $\pi/2$ flux through the triangles ($+\frac{\pi}{2}$ through up triangles and $-\frac{\pi}{2}$ through down triangles) and zero flux through the hexagons. (iv) A spin-liquid state (SL-[$\frac{\pi}{2}$, π]) with $+\pi/2$ flux through the triangles and π flux through the hexagons. (v) A uniform RVB spin-liquid state (SL-[0, 0]) with zero flux through both triangles and hexagons. This state has a spinon Fermi surface. (vi) A U(1)-Dirac spin-liquid state (SL-[0, π]) with zero flux through the triangles and π flux through the hexagons. This state has four flavors of two-component Dirac fermions.

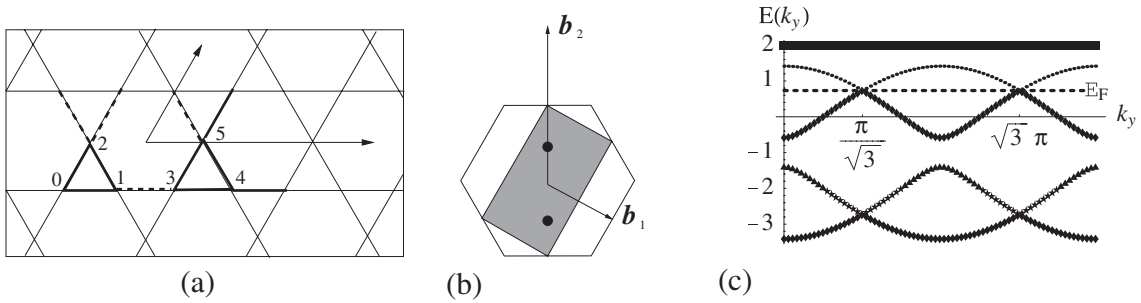

FIG. 1. (a) We choose a six-site unit cell for the Kagomé lattice. The sites are labeled $0, \ldots, 5$ as shown. Only those bonds depicted as bold solid lines (positive hopping) and bold dashed lines (negative hopping) are contained within the unit cell. (b) The Brillouin zone for the doubled unit cell (gray area), with reciprocal lattice basis vectors $\boldsymbol{b}_i$ shown. The outer hexagon is the Brillouin zone for the 3-site unit cell of a single up-pointing triangle. The positions of the Dirac nodes are denoted by the black circles. (c) Plot of the band structure of the $U(1)$-Dirac state on the line from $\boldsymbol{k} = 0$ to $\boldsymbol{k} = \boldsymbol{b}_2$ with energy in units of χJ (see text). The flat band is doubly degenerate; all others are nondegenerate. The Fermi level corresponding to one spinon per site is indicated by the dashed line.

Among the states (ii)–(v), the chiral spin-liquid SL-$[\frac{\pi}{2}, 0]$ has the lowest mean-field energy [10]. But numerical calculations [11] do not support a large chirality-chirality correlation, and Hastings [4] found SL-$[0, \pi]$ to be the state with the lowest mean-field energy among the nonchiral spin-liquid states. However, its mean-field energy is still higher than that of (ii). The above arguments are based on the $\frac{1}{N}$ expansion treatment of gauge fluctuations, which may fail when $N = 2$ in the physical case. To clarify which candidate is the lowest energy spin-liquid state, we do a Monte Carlo study on the trial projected wave functions [12].

As we mentioned, fermionic representation enlarges the Hilbert space. One way to treat the unphysical states is to do a projection by hand. Given a mean-field ground state wave function $|\Psi_{\text{mean}}(\chi_{ij})\rangle$ with mean-field parameters χ_{ij}, the projected wave function $|\Psi_{\text{prj}}(\chi_{ij})\rangle = P_D|\Psi_{\text{mean}}(\chi_{ij})\rangle$ is a physical state; here $P_D = \prod_i (1 - n_{i\uparrow}n_{i\downarrow})$ is the projection operator ensuring one fermion per site. The calculation of energy $\langle\Psi_{\text{prj}}|H|\Psi_{\text{prj}}\rangle$ can be implemented by a Monte Carlo approach with power law complexity, which means that one can do a fairly large lattice [12]. We note that states related by a global transformation $\chi_{ij} \rightarrow -\chi_{ij}^*$ represent the same spin wave function after projection. This is a special case of the $SU(2)$ gauge symmetry [13].

For the model of Eq. (1), we did the Monte Carlo calculation for energies of projected spin-liquid states on lattices with 8×8 and 12×12 unit cells (each unit cell has 3 sites). We chose mixed boundary conditions, i.e., periodic along one Bravais lattice vector, and antiperiodic along the other Bravais lattice vector. The results are summarized in Table I.

We found that the U(1)-Dirac state [the *projection* of the mean-field state (vi)] has the lowest energy, which is $-0.429J$ per site. Note that these results change the order of mean-field energies of the spin liquids (ii)–(vi), where the chiral spin liquid (ii) was found to be of the lowest energy. In Table II we list the estimates of the ground state energy by various methods. It is striking that even though the projected U(1)-Dirac state has *no variational parameter*, it has an energy which is even lower than some numerical estimates of ground state energy. Furthermore, its energy is very close to the exact diagonalization result when extrapolated to large sample size. Thus we propose it to be the ground state of the spin-1/2 nearest neighbor Heisenberg model on the Kagomé lattice.

Hastings [4] proposed a neighboring VBS ordered state as an instability of the U(1)-Dirac state. This state can be obtained by giving the fermions nonchiral masses. In particular, he proposed a VBS state with a 2×2 expansion of the unit cell. The 12 hopping parameters on the boundary of the star of David (six triangles surrounding the hexagon) have amplitude χ_1, while all other hoppings have amplitude χ_2. Our numerical calculations show that this VBS ordered state has higher energy (see Table III), so the U(1)-Dirac state is stable against VBS ordering. Another neighbor state of the U(1)-Dirac spin liquid discussed by Hastings [4] is obtained by giving the fermions chiral masses. The resulting state is a chiral spin liquid with broken time-reversal symmetry, and has θ flux through the triangles and $(\pi - 2\theta)$ flux through the hexagons [if $\theta = 0$ the state goes back to the U(1)-Dirac state]. In Table III we also show that nonzero θ increases the energy.

To determine whether the U(1)-Dirac state is a stable phase, we start with its effective theory

TABLE I. For all candidate projected spin liquids, we list the energy per site in units of J. The U(1)-Dirac state SL-$[0, \pi]$ is the lowest energy state, and its energy is even lower than some numerical estimates of the ground state energy (see Table II).

Spin liquid	$8 \times 8 \times 3$ lattice	$12 \times 12 \times 3$ lattice
SL-$[\frac{\pi}{2}, 0]$	−0.4010(1)	−0.4010(1)
SL-$[\pm\frac{\pi}{2}, 0]$	−0.3907(1)	−0.3910(1)
SL-$[\frac{\pi}{2}, \pi]$	−0.3814(1)	−0.3822(1)
SL-$[0, 0]$	−0.4115(1)	−0.4121(1)
SL-$[0, \pi]$	−0.42866(2)	−0.42863(2)

TABLE II. We list the previous estimates for ground state energy in units of J.

Method	Energy per site
Exact diagonalization [11]	−0.43
Coupled cluster method [14]	−0.4252
Spin-wave variational method [15]	−0.419

$$S = \int dx^3 \Big[\frac{1}{g^2} (\varepsilon_{\lambda\mu\nu}\partial_\mu a_\nu)^2 + \sum_\sigma \bar{\psi}_{+\sigma}(\partial_\mu - i a_\mu)\tau_\mu \psi_{+\sigma} + \sum_\sigma \bar{\psi}_{-\sigma}(\partial_\mu - i a_\mu)\tau_\mu \psi_{-\sigma} \Big] + \cdots, \quad (3)$$

where the first term comes from integrating out some higher energy fermions, and $\cdots$ represents other terms that are generated by interaction. The massless Dirac fermions in the effective theory come from the gapless nodal spinons in the mean-field theory. The two-component Dirac spinor fields are denoted by $\psi_{\pm\sigma}$, where $\pm$ label the two inequivalent nodes and σ the up or down spins. Also, $\bar{\psi}_{\pm\sigma} = \psi^\dagger_{\pm\sigma}\tau^3$, and the τ_μ are Pauli matrices. The massless fermions lead to an algebraic spin liquid [5,6]. The stability of the U(1)-Dirac state can now be determined by examining the $\cdots$ terms: if $\cdots$ terms contain no relevant perturbations—that is, if all relevant perturbations are forbidden by microscopic symmetries—then the U(1)-Dirac state can be stable.

The potential relevant terms are the 16 gauge-invariant, spin-singlet bilinears of $\psi_{\pm\sigma}$. To see if those bilinears are generated by interaction or not, we need to study how lattice symmetries are realized in the effective theory (4). Because spinons are not gauge invariant, lattice symmetry is realized in the effective theory as a projective symmetry, described by a PSG. This means that the realization of lattice symmetry includes nontrivial gauge transformations. For example, translation $T_{\boldsymbol{R}}$ by a Bravais lattice vector $\boldsymbol{R}$ acts on the spinons by $T_{\boldsymbol{R}}$: $f_{i\alpha} \to g(i, \boldsymbol{R}) f_{i'\alpha}$, where i' is the image of the site i, and $g(i, \boldsymbol{R}) = \pm 1$ is a position-dependent gauge transformation. Upon diagonalizing the mean-field Hamiltonian for the U(1)-Dirac state and focusing on the low-energy excitations near the Dirac nodes (see below), the action of $T_{\boldsymbol{R}}$ (and other symmetries) on the fermions $\psi_{\pm\sigma}$ of the effective theory can be worked out. This in turn determines how the bilinears transform under microscopic symmetries. The details of this analysis for the U(1)-Dirac state, which do not differ substantially from similar analyses of other spin liquids [5–7], will appear in an upcoming paper; here, we simply give the results.

We find that 15 of 16 bilinears are forbidden by translation symmetry and time reversal alone. The remaining bilinear, which is allowed by symmetry, is $\sum_{\pm,\sigma} \psi^\dagger_{\pm\sigma}\psi_{\pm\sigma}$. This term shifts the spinon Fermi level to make the ground state to have exactly one spinon per site. In this case, the lower three of six spinon bands are filled and the spinon Fermi level is exactly at the gapless nodal points. This analysis tells us that the U(1)-Dirac state is stable in mean-field theory (and also in a large-N treatment). Because not all scaling exponents are known in such an algebraic spin liquid, perturbations other than fermion bilinears could in principle lead to an instability. However, so far, the variational wave function analysis suggests that this is not the case and that the U(1)-Dirac state is stable.

Now we study the U(1)-Dirac spin liquid on the mean-field level. The U(1)-Dirac mean-field state is defined as the ground state of the following tight-binding spinon Hamiltonian: $H_{\text{mean}} = J\sum_{\langle ij\rangle} \chi_{ij} f^\dagger_{j\alpha} f_{i\alpha} + \text{H.c.}$. All χ_{ij} have the same magnitude and they produce zero flux through the triangles and π flux through the hexagons.

Although the U(1)-Dirac state does not break translation symmetry (because the translated state differs from the original state only by a gauge transformation), the unit cell has to be doubled to work out the mean-field spinon band structure. One can fix a gauge in which all hoppings are real as shown in Fig. 1(a). In this gauge the Dirac nodes are found to be at $\boldsymbol{k} = (0, \pm \frac{\pi}{\sqrt{3}a})$ as shown in Fig. 1(b) and 1(c), where a is the Kagomé unit cell spacing, i.e., twice the nearest neighbor distance. These are isotropic Dirac nodes; i.e., the Fermi velocity is the same in all directions. In the extended zone scheme, the Dirac nodes form a triangular lattice in momentum space with lattice spacing $\frac{2\pi}{\sqrt{3}a}$. The positions of the Dirac nodes are gauge dependent, but the momentum vectors connecting any two Dirac nodes are gauge invariant. Because the spinon excitations are gapless at the nodal points, we expect the spin-1 excitations of the U(1)-Dirac spin liquid are also gapless at zero momentum and those momenta connecting two Dirac nodes.

For the $ZnCu_3(OH)_6Cl_2$ compound, the Heisenberg coupling was estimated to be $J \approx 300$ K [1], and one can

TABLE III. We list the energy per site in unit of J for possible instabilities of the U(1)-Dirac spin liquid, which were discussed in Ref. [4] (see text). Both VBS order and chiral spin liquid increase the energy. Note that both the VBS and chiral spin-liquid states are obtained by continuous deformations of the U(1)-Dirac wave function; because we are checking local stability, the parameters used here correspond to small deformations, and the energy differences are rather small.

State	$8 \times 8 \times 3$ lattice	$12 \times 12 \times 3$ lattice
U(1)-Dirac spin liquid	−0.42866(2)	−0.42863(2)
VBS state ($\lvert\chi_1/\chi_2\rvert = 1.05$)	−0.42848(2)	−0.42844(2)
VBS state ($\lvert\chi_1/\chi_2\rvert = 0.95$)	−0.42846(2)	−0.42846(2)
Chiral spin liquid ($\theta = 0.05$)	−0.42857(2)	−0.42853(2)

calculate the Fermi velocity at mean-field level. We find $v_F = \frac{a\chi J}{\sqrt{2}\hbar}$, where χ is the magnitude of the self-consistent mean-field parameter. Hastings [4] found $\chi = 0.221$. χ describes the renormalization of the spinon bandwidth and is not expected to be given quantitatively by the mean-field theory. Hence in the formulas below we retain χ as a parameter. We find $v_F = \frac{a\chi J}{\sqrt{2}\hbar} = 19\chi \times 10^3$ m/s.

We can also calculate the specific heat at the mean-field level. At low temperature ($k_B T \ll \chi J$), one expects a $C \propto T^2$ law because of the Dirac nodes. The coefficient is related to v_F:

$$\frac{C}{T^2} = \frac{72\zeta(3)\pi k_B^3 A}{(2\pi\hbar v_F)^2} = 1.1\chi^{-2} \times 10^{-3}\ \text{Joule/mol K}^3, \quad (4)$$

where A is the area of the 2-D system. [Note that for $ZnCu_3(OH)_6Cl_2$ compound, the unit cell spacing $a = 6.83$ Å, so $A = 2.4 \times 10^5$ m^2/mol, where mole refers to one formula unit. We also used the fact that there are four two-component Dirac fermions.]

In a magnetic field, the spinons will form a Fermi pocket whose radius is proportional to magnetic field strength. Therefore, at low temperature $k_B T \ll \mu_B B$, the specific heat is linear in T:

$$\frac{C}{T} = \frac{8\pi^3 k_B^2 A \mu_B B}{3(2\pi\hbar v_F)^2} = 0.23\chi^{-2} B \times 10^{-3}\ \text{Joule/mol K}^2,$$

where magnetic field B is in unit of Tesla. We also find in the temperature range $\mu_B B \ll k_B T \ll \chi J$,

$$C = \frac{24\pi A k_B^3 T^2}{(2\pi\hbar v_F)^2}\left[3\zeta(3) + \frac{2\ln 2}{3}\left(\frac{\mu_B B}{k_B T}\right)^2 + O(B^4)\right].$$

Keeping the lowest order correction, the specific heat has a *temperature independent* increase proportional to B^2.

$$\Delta C = \frac{16\pi \ln 2 k_B A}{(2\pi\hbar v_F)^2}(\mu_B B)^2 = 6.3\chi^{-2} B^2 \times 10^{-5}\ \text{Joule/mol K}. \quad (5)$$

This is in contrast to the specific heat shift of a local moment, which decreases with T as B^2/T^2. Equation (5) provides a way to separate the Dirac fermion contribution from that of impurities and phonons.

The gauge field also gives a T^2 contribution to the specific heat. However, in a large-N treatment this will be down by a factor of $1/N$ compared to the fermion contribution. Furthermore, the self-energy correction due to gauge fluctuations does not lead to singular corrections to the Fermi velocity [16], so the T^2 dependence of C is a robust prediction.

We notice that experiment observed that the specific heat of Kagomé compound $ZnCu_3(OH)_6Cl_2$ behaves as $C \propto T^{2/3}$ in zero magnetic field over the temperature window 106 mK $< T <$ 600 mK [1], which is enhanced from $C \propto T^2$ law. This enhancement is suppressed by a modest magnetic field [1]. Furthermore, over a large temperature range (10 K to 100 K), the spin susceptibility is consistent with Curie's law with 6% impurity local moment [3]. We propose that these impurity spins (possibly due to Cu located on the Zn sites) may be coupled to the spinons to form a Kondo type ground state with a Kondo temperature $\lesssim 1$ K, thus accounting for the large C/T and the saturation of the spin susceptibility below 0.3 K. The Kondo physics of impurities coupled to Dirac spinons is in itself a novel problem worthy of a separate study. Meanwhile, it appears to dominate the low temperature properties and obscure the true excitations of the Kagomé system. We propose that a better place to look for the Dirac spectrum may be at higher temperature (above 10 K) and as a function of magnetic field, where the impurity contributions may be suppressed and the unique signature of Eq. (4) and (5) may be tested. On the other hand, we caution that from Fig. 1(c), the spinon spectrum deviates from linearity already at a relatively low-energy scale ($\sim 0.5\chi J$). Our theory also predicts a linear T spin susceptibility of $k_B T \ll \chi J$. Knight shift measured by Cu NMR is the method of choice to separate this from the impurity contribution.

Finally we remark on a possible comparison with exact diagonalization studies which found a small spin gap of $\sim \frac{J}{20}$ and a large number of low-energy singlets [11]. It is not clear whether these results can be reconciled with a $U(1)$-Dirac spin liquid. Here we simply remark that in a finite system the Dirac nodes can easily produce a small triplet gap and that the gauge fluctuations may be responsible for low-energy singlet excitations.

We thank J. Helton and Y. S. Lee for helpful discussions. This research is supported by NSF Grants No. DMR-0433632 and No. DMR-0517222.

[1] J. S. Helton *et al.*, cond-mat/0610539 [Phys. Rev. Lett. (to be published)].
[2] O. Ofer *et al.*, cond-mat/0610540.
[3] P. Mendels *et al.*, Phys. Rev. Lett. **98**, 077204 (2007).
[4] M. B. Hastings, Phys. Rev. B **63**, 014413 (2000).
[5] X.-G. Wen, Phys. Rev. B **65**, 165113 (2002).
[6] M. Hermele, T. Senthil, M. P. A. Fisher, P. A. Lee, N. Nagaosa, and X.-G. Wen, Phys. Rev. B **70**, 214437 (2004).
[7] Y. Ran and X.-G. Wen, cond-mat/0609620.
[8] G. Baskaran, Z. Zou, and P. Anderson, Solid State Commun. **63**, 973 (1987).
[9] G. Kotliar and J. Liu, Phys. Rev. B **38**, 5142 (1988).
[10] J. Marston and C. Zeng, J. Appl. Phys. **69**, 5962 (1991).
[11] C. Waldtmann *et al.*, Eur. Phys. J. B **2**, 501 (1998).
[12] C. Gros, Ann. Phys. (N.Y.) **189**, 53 (1989).
[13] P. Lee, N. Nagaosa, and X.-G. Wen, Rev. Mod. Phys. **78**, 17 (2006).
[14] D. J. J. Farnell, R. F. Bishop, and K. A. Gernoth, Phys. Rev. B **63**, 220402 (2001).
[15] L. Arrachea, L. Capriotti, and S. Sorella, Phys. Rev. B **69**, 224414 (2004).
[16] D. H. Kim, P. A. Lee, and X.-G. Wen, Phys. Rev. Lett. **79**, 2109 (1997).